Diffusion-Weighted Echo-Planar MR Imaging of Primary Parotid Gland Tumors: Is a Prediction of Different Histologic Subtypes Possible?

C.R. Habermann, C. Arndt, J. Graessner, L. Diestel, K.U. Petersen, F. Reitmeier, J.O. Ussmueller, G. Adam and M. Jaehne

AJNR Am J Neuroradiol 2009, 30 (3) 591-596
doi: https://doi.org/10.3174/ajnr.A1412
http://www.ajnr.org/content/30/3/591

ORIGINAL RESEARCH

Diffusion-Weighted Echo-Planar MR Imaging of Primary Parotid Gland Tumors: Is a Prediction of Different Histologic Subtypes Possible?

C.R. Habermann
C. Arndt
J. Graessner
L. Diestel
K.U. Petersen
F. Reitmeier
J.O. Ussmueller
G. Adam
M. Jaehne

BACKGROUND AND PURPOSE: Our aim was to determine the value of echo-planar diffusion-weighted MR imaging (epiDWI) in differentiating various types of primary parotid gland tumors.

MATERIALS AND METHODS: One hundred forty-nine consecutive patients with suspected tumors of the parotid gland were examined with an epiDWI sequence by using a 1.5T unit. Image analysis was performed by 2 radiologists independently, and the intraclass correlation coefficient was computed. Histologic diagnosis was obtained in every patient. For comparison of apparent diffusion coefficients (ADCs), a paired 2-tailed Student *t* test with a Bonferroni correction was used.

RESULTS: In 136 patients, a primary parotid gland tumor was confirmed by histology. Among the observers, a high correlation was calculated (0.98). ADC values of pleomorphic adenomas were significantly higher than those of all other entities, except for myoepithelial adenomas ($P = .054$). ADC values of Warthin tumors were different from those of myoepithelial adenomas, lipomas, and salivary duct carcinomas ($P < .001$, 0.013, and .037, respectively). Mucoepidermoid carcinomas, acinic cell carcinomas, and basal cell adenocarcinomas were not differentiable from Warthin tumors ($P = .094$, .396, and .604, respectively).

CONCLUSION: epiDWI has the potential to differentiate pleomorphic adenoma and myoepithelial adenomas from all other examined entities. Due to an overlap not only within the group of benign and malignant lesions but also between groups, diagnoses should not be addressed on the basis of ADC values solely. Therefore, further studies combining DWI, morphologic criteria, and probably other MR imaging techniques seem warranted.

Among all human organs, salivary glands offer the largest variety of different histologic types and subtypes of primary neoplasms, most of them arising in the parotid glands.[1] Therefore, the management of tumors of the salivary glands requires a detailed understanding of the anatomy and pathologic processes affecting these glands.[2,3] Most important for choosing the appropriate surgical approach regarding a primary tumor of the salivary glands is not only the preoperative differentiation between a benign or malignant lesion but also the determination of the exact histologic subtype among benign or malignant lesions.[2-5] Whereas the risk for local recurrence in Warthin tumors treated by enucleation is approximately 2%, the risk for local recurrence in pleomorphic adenomas treated in the same manner is reported to be approximately 85%.[3,4,6-8] This perception leads to different surgical approaches among not only benign but also malignant lesions.[4,5,7] Fine-needle aspiration cytology (FNAC) proved to be a useful and reliable tool in the preoperative diagnosis of salivary gland masses when performed by a radiologist or a clinician.[1,9-13] In contrast, Das et al[14] reported, in a study of 712 patients, a diagnostic accuracy reaching only from 80% to 91.1%.

A risk of FNAC might be a possible spread of tumor cells, which can lead to a higher likelihood of local recurrence, especially in pleomorphic adenomas and malignant lesions. Additionally, the differentiation of a few benign and malignant lesions might be not only difficult but also impossible.[14,15] For instance, pleomorphic adenomas of variable histologic patterns can be mistaken for several other types of tumors, such as mucoepidermoid carcinoma or adenoid cystic carcinoma.[1] Furthermore, a differentiation between a basal cell adenoma and a basal cell adenocarcinoma based solely on a FNAC is usually not possible.[14,16]

Therefore, several MR imaging–based techniques have been evaluated for the diagnosis of benign and malignant salivary gland tumors.[17-31] In contrast to FNAC, a noninvasive examination such as MR imaging might provide a diagnosis and also stage the disease. Among the evaluated image-based techniques, diffusion-weighted imaging (DWI) seems to have the highest potential to determine different histologic subtypes of salivary gland tumors noninvasively.[18,19,31,32] In unison, the mentioned authors referred to the high potential of DWI for differentiating benign and malignant lesions or, furthermore, determining different histologic subtypes within the 2 groups. The major drawback of the mentioned studies is the limited number of histologic subtypes of primary salivary gland tumors, which might lead to an overestimation of this technique.

The purpose of our prospective study was to investigate the potential of echo-planar DWI (epiDWI) in differentiating various entities of parotid gland tumors.

Materials and Methods

Subjects

This prospective study was conducted in accordance with the recommendations of the local ethics committee that approved it. Written

Received August 8, 2008; accepted after revision October 17.

From the Department of Diagnostic and Interventional Radiology (C.R.H., C.A., L.D., G.A.), Diagnostic Center; Department of Psychiatry and Psychotherapy (K.U.P.), Center of Psychosocial Medicine; and Department of Oto-, Rhino-, Laryngology (F.R., M.J.), Center for Head Care and Dermatology, University Medical Center Hamburg-Eppendorf, Hamburg, Germany; Siemens Healthcare (J.G.), Hamburg, Germany; and Center of Oto-, Rhino-, Laryngology Regensburg (J.O.U.), Regensburg, Germany.

Please address correspondence to Christian R. Habermann, MD, University Medical Center, Diagnostic Center, Department of Diagnostic and Interventional Radiology, Martinistr. 52, 20246 Hamburg, Germany; e-mail: c.habermann@uke.uni-hamburg.de

DOI 10.3174/ajnr.A1412

informed consent for participation in this study was signed by all included patients.

Between February 2003 and January 2008, 149 consecutive patients (67 females, 82 males; age range, 17–90 years; mean age, 57.2 years ± 12.6) with a clinically suspected primary tumor of the parotid gland were examined prospectively before surgery. Before MR imaging, all patients underwent sonography to confirm the suspected clinical diagnosis. As part of the study protocol, in none of the included patients was a fine-needle aspiration performed before MR imaging. All patients underwent surgery, and in all cases, histologic diagnosis was available. The maximal period between MR imaging and surgery was 15 days (range, 1–15 days; mean, 5.7 ± 2.3 days).

MR Imaging Protocol

All examinations were performed on a 1.5T superconducting MR imaging system with a 30 mT/m maximum gradient capability and a maximum slew rate of 125 mT/m/ms (Magnetom Symphony; Siemens Medical Solutions, Forchheim, Germany). The lower part of the circularly polarized (CP) head coil and a standard 2-element CP neck array coil were used. The flexibility of the neck array coil allowed positioning of the N1 element (the upper part of the coil) right next to the parotid glands. Initially, for anatomic localization of the parotid gland, an axial T1-weighted spin-echo sequence (TR, 500 ms/TE, 14 ms) was performed by using a matrix of 192 × 512, an FOV of 210 × 280 mm (pixel size, 1.09 × 0.55 mm), a section thickness of 5 mm with an intersection gap of 1.25 mm, and 3 signals averaged. The acquisition time of this sequence was 1 minute 45 seconds.

As a T2-weighted sequence, 3D true fast imaging with steady-state precession (true FISP) (TR, 700 ms/TE, 2.29 ms) with spectral fat saturation was performed by using a matrix of 256 × 256, an FOV of 160 × 160 mm (pixel size 0.6 × 0.6 mm), a section thickness of 2.5 mm, and 3 signals averaged. The acquisition time of this sequence was 1 minute 44 seconds. Instead of a T2-weighted spin-echo sequence, this one was performed to combine the T2 image impression and improve the visualization of the excremental ducts. Hence, this sequence was a compromise between a morphologic T2-weighted sequence and the heavily T2-weighted sequence to get a T2-weighted image impression of the glands and to evaluate the excremental ducts for possible additional pathologies.

The resulting images were analyzed for morphologic alterations, such as metal artifacts from dental implants and localization of the tumor, to ensure proper coverage of the entire tumor, by the following epiDWI sequence in consensus by 2 radiologists (C.R.H. and T.R., with 12 and 2 years of experience in the field of radiology, respectively). Thereafter, an axial epiDWI sequence (TR, 1500 ms; TE, 77 ms) was performed with a matrix of 119 × 128, an FOV of 250 × 250 mm (pixel size, 2.10 × 1.95 mm), 6 excitations, and a section thickness of 5 mm with an intersection gap of 1 mm. A parallel imaging technique (modified sensitivity encoding) with an acceleration factor of 2 with 12 additional lines for self-calibrating was applied. A bandwidth of 1502 Hz/pixel was used, and 12 sections were acquired. The b factors used were 0 s/mm^2, 500 s/mm^2, and 1000 s/mm^2. Fat suppression was achieved by placing the frequency-selective radio-frequency pulse before the pulse sequence. The automatic 3D shim routine of the magnet used the section block as the shim volume, and shimming was performed directly before the sequence was started. The total acquisition time of this sequence was 1 minute 14 seconds.

Image Analysis

For each epiDWI sequence, a pixel-by-pixel apparent diffusion coefficient (ADC) map was automatically calculated, with the gray value of the pixel linearly corresponding to the ADC value expressed in square millimeters per second. The ADC values were calculated by using a least-square solution of the following system of equations: $S(i) = S_O \times \exp(-b_i \times ADC)$, where S(i) is the signal intensity measured on the i^{th} b factor and b_i is the corresponding b factor image.[33] S_O is a variable estimating the exact signal intensity for a b factor of 0 s/mm^2.[34]

Data were digitally transferred to the analyzing software MRIcro 1.4 (Chris Rorden, University of Nottingham, Great Britain; http://www.sph.sc.edu/comd/rorden), which lists every pixel intensity of each ADC map in a single region-of-interest output file per patient. The delineation of tumors on ADC maps and subsequently the ADC computation were performed by 2 investigators (C.R.H. and L.D.), independently. An irregular region of interest was placed manually on ADC maps covering the entire tumor of every patient. This procedure was performed on all ADC maps where the tumor was visible, depending on the craniocaudal tumor extension. The localization of every single region of interest was confirmed by using the morphologic T1- and T2-weighted sequences. In a first step, the mean ADC value per region of interest and per patient was computed. The following analyses were based on the mean of each patient's mean values. Only entities with at least ≥2 examined patients were included in the further statistical evaluation, to ensure statistical accuracy. Subsequently, each tumor size was measured in consensus by 2 radiologists (C.R.H. and L.D.) in every patient by using the software eFilm 2.1.2 (Merge Healthcare, Milwaukee, Wis) based on T2-weighted images.

Statistical Analysis

All statistical analyses were computed with the Statistical Package for the Social Sciences, Version 13.0.1 (SPSS, Chicago, Ill). ADC values for each histologic subtype were achieved by taking the mean of the separate mean values of each tumor per patient. For comparison of the different histologic types of parotid gland tumors, an unpaired 2-tailed Student *t* test with a Bonferroni correction for multiple testing was used, and a $P < .05$ was considered to indicate statistical significance. Regarding the ADC determinations by the 2 radiologists, an intraclass correlation coefficient was computed to evaluate interobserver variability and a correlation >0.8 was high.

Results

In 145 of 149 patients, a single 1-sided lesion was detected within the right ($n = 67$) or left ($n = 78$) parotid gland. In 4 patients, 2 lesions (right side, $n = 1$; left side, $n = 3$) were visible on MR images and confirmed by surgery and histologic work-up. In the 4 mentioned patients with 2 lesions within a parotid gland, pathology confirmed Warthin tumors. For further evaluation, only the larger lesion was included in the study.

epiDWI depicted the parotid glands of all patients, and in all patients, the delineation of the lesion was possible on ADC maps but additionally confirmed on the morphologic T1- and T2-weighted sequences. In 13 patients, the suspected lesions within the parotid gland proved to represent involvement from nonparotideal malignancies ($n = 9$, lymphoma metastases) or inflammatory pseudolesions ($n = 4$) and, therefore, were excluded from further evaluation.

The histopathologic distributions of primary parotid gland

Table 1: Histopathologic diagnoses of examined primary salivary gland tumors

Diagnosis	No. of Lesions (n = 136)
Pleomorphic adenoma	43
Warthin tumor	32
Myoepithelial adenoma	6
Lipoma	3
Basal cell adenoma	1
Cystadenoma	1
Inverted ductal papilloma	1
Mucoepidermoid carcinoma	16
Salivary duct carcinoma	11
Acinic cell carcinoma	10
Basal cell adenocarcinoma	9
Adenoid cystic carcinoma	1
Epithelial-myoepithelial carcinoma	1
Carcinoma ex pleomorphic adenoma	1

Table 2: Mean ADC values of all histologically proved entities of parotid gland tumors (n = 136)*

Diagnosis	Mean ADC values ± SD (95% CI) ($\times 10^{-3}$ mm^2/s)
Pleomorphic adenoma (n = 43)	2.09 ± 0.16 (2.03–2.14)
Warthin tumor (n = 32)	0.89 ± 0.16 (0.82–0.96)
Myoepithelial adenoma (n = 6)	1.86 ± 0.18 (1.83–1.91)
Lipoma (n = 3)	0.62 ± 0.21 (0.54–0.76)
Basal cell adenoma (n = 1)	1.23
Cystadenoma (n = 1)	2.29
Inverted ductal papilloma (n = 1)	1.99
Mucoepidermoid carcinoma (n = 16)	1.05 ± 0.03 (0.97–1.14)
Salivary duct carcinoma (n = 11)	1.10 ± 0.09 (0.89–1.31)
Acinic cell carcinoma (n = 10)	0.79 ± 0.33 (0.68–0.88)
Basal cell adenocarcinoma (n = 9)	0.96 ± 0.29 (0.71–1.12)
Adenoid cystic carcinoma (n = 1)	0.87
Epithelial-myoepithelial carcinoma (n = 1)	0.92
Carcinoma ex pleomorphic adenoma (n = 1)	1.14

Note:—CI indicates confidence interval; ADC, apparent diffusion coefficient.
* In case of a single tumor, SD and 95% CI were not calculated.

tumors within the remaining 136 patients (62 women, 74 men; age range, 33–90 years; mean age, 59.2 ± 14.9 years) are given in Table 1. The mean tumor size was 2.1 ± 0.6 cm (range, 0.4–3.2 cm). The highest ADC value among all tumor entities was calculated for a solitary cystadenoma (2.29×10^{-3} mm^2/s), which showed a higher ADC value than pleomorphic adenomas (2.09×10^{-3} mm^2/s ± 0.16×10^{-3} mm^2/s) (Table 2 and Fig 1). On the basis of the mean of the ADC values, pleomorphic adenomas were distinguishable from all other examined subtypes, except for myoepithelial adenomas (P = .054, Fig 2). Mean ADC values from Warthin tumors (0.89×10^{-3} mm^2/s ± 0.16×10^{-3} mm^2/s), as the second most common tumor of parotid glands, were statistically significantly different from those of myoepithelial adenomas, lipomas, and salivary duct carcinomas ($P < .001$, .013, and .037, respectively; Fig 3). In contrast, mucoepidermoid carcinomas, acinic cell carcinomas, and basal cell adenocarcinomas were not differentiable from Warthin tumors on the basis of ADC values solely (P = .094, .396, and .604, respectively). The detailed significance levels are given in Table 3.

For the ADC computation, a high correlation was calculated between the 2 observers, with an intraclass correlation coefficient of 0.98 ($P < .001$).

Discussion

We investigated the potential of epiDWI in differentiating various entities of parotid gland tumors. Our results demonstrate that there is not only an overlap within the group of benign and malignant primary tumors of the parotid gland but also an overlap between benign and malignant tumors.

These results are in slight contrast to other studies dealing with this specific topic.[18,19,31,32] In a recently published study by Eida et al,[18] 31 consecutive patients with a single tumor in the parotid or submandibular gland were evaluated. The authors concluded that ADC may provide preoperative tissue characterization of salivary gland tumors by using different b factors (500 and 1000 s/mm^2). In contrast to our study, the predictive ability of the MR imaging criteria based on the ADC levels was assessed by dividing the calculated values in 4 groups (extremely low, low, intermediate, or high). Additionally, ADC levels were calculated from different areas of each tumor. Regarding the areas with extremely high ADCs, the difference between benign and malignant lesions was statistically significant. The authors did not provide absolute ADC values for different entities, even though, by using an alternative evaluation method, this study offers very promising results. The major difficulty of this study might be to implement the method of determining different tumor areas within a single tumor in a clinical routine setting. Parotid glands and, moreover, submandibular glands are small organs; a virtual fragmentation of small lesions within a small organ might allow the application of this evaluation technique only in larger lesions.

A comparable evaluation method was performed by Matsushima et al[21] in 32 patients with salivary gland tumors (17 benign, 15 malignant). Considering different degrees of extracellular components, they made comparisons of mean ADC values between benign and malignant tumors and among tumors showing different degrees of extracellular components. In contrast to Eida et al,[18] no significant difference in mean ADC values was found between benign and malignant tumors, and the mean ADC values increased with the degree of extracellular components. On the basis of these results, Matsushima et al concluded that ADC values alone are not sufficient to differentiate benign from malignant salivary gland tumors.

In a study provided by Yoshino et al[31] (b factors, 0 and 771 s/mm^2), the provided ADC value for a pleomorphic adenoma (n = 1) was 1.99×10^{-3} mm^2/s and for Warthin tumors (n = 2) was 0.89×10^{-3} mm^2/s and thus similar to the values observed in our study. In contrast, the ADC value for an acinic cell carcinoma was much higher ($1.38–2.11 \times 10^{-3}$ mm^2/s). This remarkable difference regarding ADC values of acinic cell carcinomas might be explained by the fact that in the single acinic cell carcinoma observed by Yoshino et al, a cystic component was observed, which might lead to a substantial increase of ADC. In our study, all acinic cell carcinomas (n = 10) presented as solid tumors. However, this study was not focused on tumors (n = 5) and might be, therefore, categorized as preliminary, with regard to this special topic.[31]

In another study, including 45 patients, the drawn conclusion was very promising (b factors, 0, 500, and 1000 s/mm^2).[19] Only an overlap within the malignant tumors was observed and additionally between myoepithelial adenomas (n = 3) and salivary duct carcinomas (n = 3). Pleomorphic adenomas were distinguishable from all 6 other examined entities solely

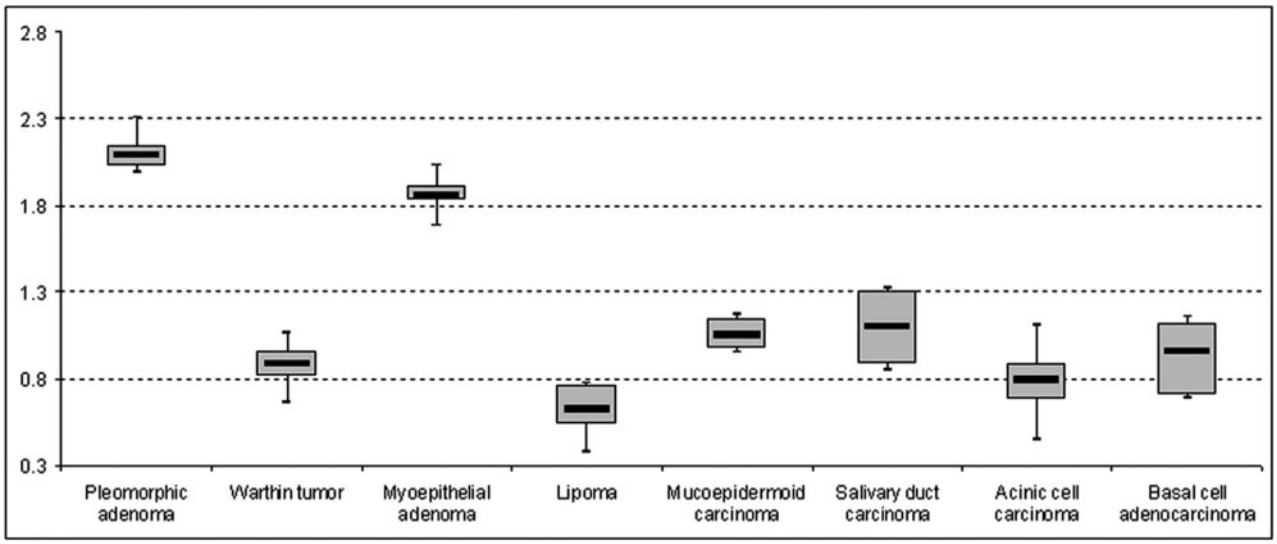

Fig 1. The boxplots demonstrate the mean value, 95% confidence interval (CI), and minimum and maximum values for each tumor entity with a number of patients >1. The central line of each boxplot indicates the mean value, whereas the range of the box displays the 95% CI. The whiskers represent the minimal and maximal values (unit of the vertical axis: $\times 10^{-3}$ mm^2/s).

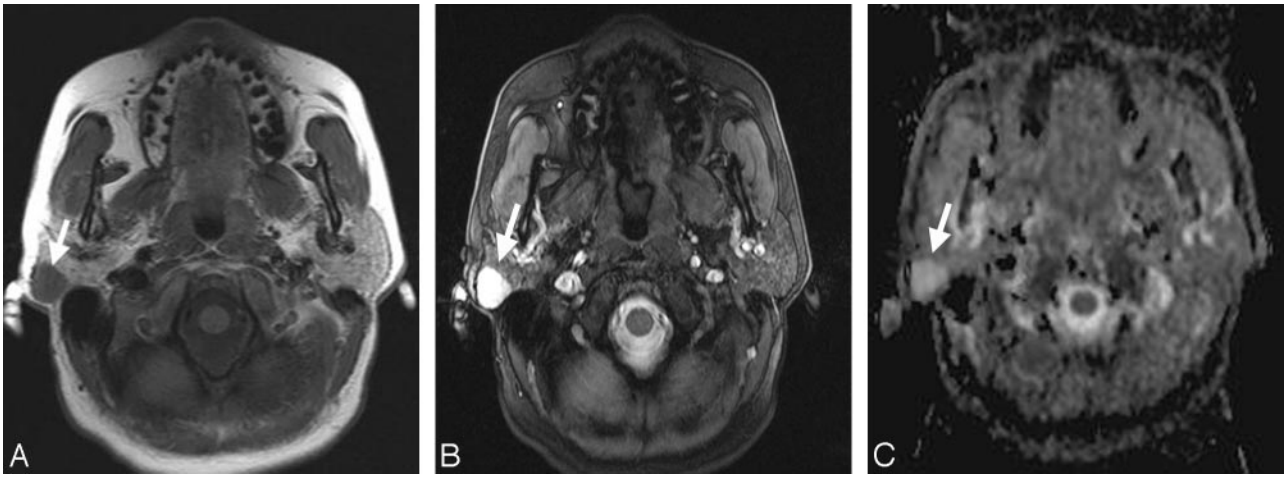

Fig 2. *A*, Transverse T1-weighted spin-echo MR image (TR, 500 ms; TE, 14 ms) from a 69-year-old male patient with a histologically proved pleomorphic adenoma within the right parotid gland (*arrow*). The mass shows muscle-isointense signal intensity. *B*, The corresponding T2-weighted 3D true FISP (TR, 700 ms; TE, 2.29 ms) image has a bright lesion within the right parotid gland (*arrow*). *C*, The corresponding ADC map shows an easily detectable bright signal intensity of the lesion (mean ADC value: 2.14×10^{-3} mm^2/s; *arrow*).

on the basis of the calculated ADC values. In our study, pleomorphic adenomas were also distinguishable from all other entities, except for myoepithelial adenomas. This drawback focused on pleomorphic adenoma could be considered insignificant because both lesions were benign. From the point of view of a head and neck surgeon, this disadvantage has a higher impact, caused by the fact that pleomorphic adenomas have a risk of malignant transformation (carcinoma ex pleomorphic adenoma) and the surgical approach has to be much more aggressive due to the high risk of recurrence (eg, lateral or complete parotid resection) with a higher risk of facial nerve injury.[35] Otherwise, myoepithelial adenomas have an explicitly lower risk of malignant transformation or recurrences and can, therefore, be resected more conservatively.[36]

Warthin tumors, as the second most common benign tumors of parotid glands, are treated much more conservatively than pleomorphic adenomas and, of course, all malignant lesions.[6,37] A Warthin tumor treated by enucleation has an expected recurrence rate of only 2%.[6] Therefore, differentiation from malignant lesions would be very helpful with respect to the surgical approach. In our study, the ADC value for Warthin tumors was 0.89×10^{-3} $mm^2/s \pm 0.16\ 10^{-3}$ mm^2/s. This ADC value is very close to that in all other studies dealing with this topic, ranging from 0.72×10^{-3} mm^2/s to 0.96×10^{-3} mm^2/s.[19,31,38] Focused on Warthin tumors, Ikeda et al[38] calculated the average ADC value of Warthin tumors (0.96×10^{-3} mm^2/s; $n = 19$) to be significantly lower than that in all included malignant lesions (1.19×10^{-3} mm^2/s; $n = 17$). However, the ADC values for Warthin tumors ranged from 0.72×10^{-3} mm^2/s to 1.17×10^{-3} mm^2/s, showing an overlap with examined malignant lesions (0.79×10^{-3} mm^2/s to 1.65×10^{-3} mm^2/s). These results strongly support our findings, proving a limited value of ADC-based tumor differentiation focused on Warthin tumors in an individual case.

To a certain extent, epiDWI seems to have the potential to differentiate primary parotid gland lesions. However, this di-

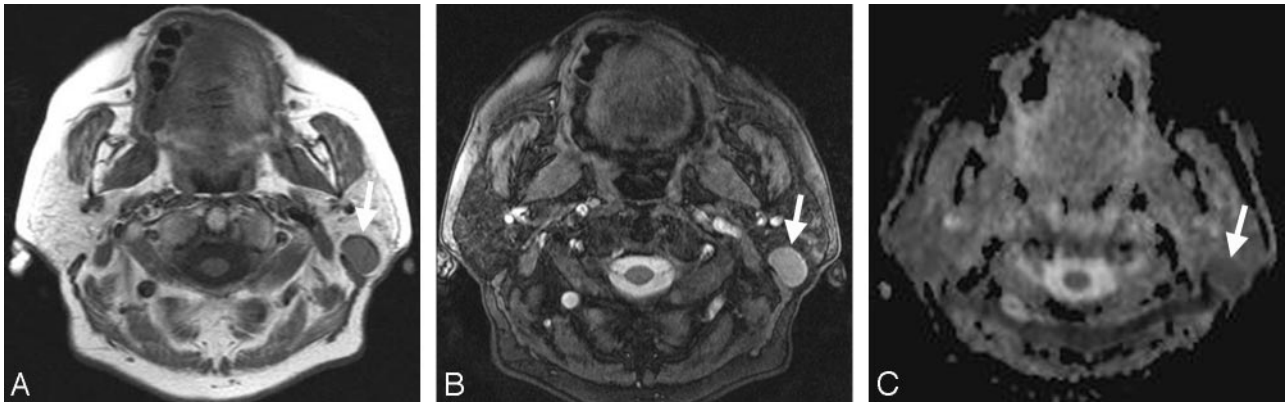

Fig 3. *A*, Transverse T1-weighted spin-echo MR image (TR, 500 ms; TE, 14 ms) from a 49-year-old female patient with a histologically proved Warthin tumor in the left parotid gland (*arrow*). *B*, The T2-weighted image (3D true FISP; TR, 700 ms; TE, 2.29 ms) also shows a bright signal intensity of the lesion (*arrow*) with a lesser extent but appearance similar to that of the pleomorphic adenoma in Fig 2*B*. *C*, On the basis of ADC maps, the difference between the pleomorphic adenoma in Fig 2*C* and the Warthin tumor shown (*arrow*) becomes obvious (mean ADC value: 0.85×10^{-3} mm^2/s).

Table 3: Level of significance of calculated mean ADC values comparing all observed entities ($n > 1$)

	Warthin Tumors	Myoepithelial Adenomas	Lipomas	Mucoepidermoid Carcinomas	Salivary Duct Carcinomas	Acinic Cell Carcinomas	Basal Cell Adenocarcinomas
Pleomorphic adenomas	<.001	.054*	<.001	<.001	<.001	<.001	<.001
Warthin tumors		<.001	.013	.094*	.037	.396*	.604*
Myoepithelial adenomas			.009	.133*	.014	.032	.082*
Lipomas				.024	.022	.48*	.222*
Mucoepidermoid carcinomas					.430*	.246*	.569*
Salivary duct carcinoma						.195*	.446*
Acinic cell carcinomas							.616*

* Non-statistically significant differences.

agnostic approach has to be reviewed very carefully. A larger number of observed lesions will provide more different histologic subtypes when dealing with organs offering a wide histologic variety of primary tumors. Most likely, this fact will lead to restrictions dealing with this technique. The presented study offers the largest number of primary parotid gland tumors and different histologic subtypes within the literature and, in contrast to most other studies, an overlap regarding the ADC values from Warthin tumors and 3 different malignant subtypes of parotid gland lesions. With regard to our results, the conclusions given in the literature should be relativized. In a recent published study by Prades et al,[26] the offered results for determining whether a tumor is benign or malignant on the basis of the morphologic appearance are very promising and might be improved by combining morphologic features and DWIs in a diagnostic noninvasive approach.[39] This is especially promising with regard to the differentiation of pleomorphic adenomas, which were diagnosed with an accuracy of 83%, and Warthin tumors, which were diagnosed with an accuracy of 85%, on the basis of the morphologic appearance.[26]

The main limitation of our study is that not every examined tumor subgroup was available in a satisfying number of patients; therefore, the ADC values might vary after including more patients for every subgroup. Furthermore, the number of malignancies is still very limited ($n = 49$). However, salivary gland tumors are rare, and to our knowledge, our study provides the largest number of patients with parotid gland tumors examined with epiDWI within the literature.

Conclusions

epiDWI has the potential to differentiate pleomorphic adenoma and myoepithelial adenomas from all other examined entities. Due to an overlap not only within the group of benign and malignant lesions but also an overlap between these groups, diagnoses should not be addressed on the basis of ADC values solely. Therefore, further studies combining DWI, morphologic criteria, and probably other MR imaging techniques seem to be warranted.

References

1. Seifert G. *Histoligical Typing of Salivary Gland Tumors.* 2nd ed Berlin, Germany: Springer-Verlag; 1991:24–54
2. Scianna JM, Petruzzelli GJ. **Contemporary management of tumors of the salivary glands.** *Curr Oncol Rep* 2007;9:134–38
3. Swoboda H, Franz P. **Salivary gland tumors: clinical aspects and therapy** [in German]. *Radiologe* 1994;34:232–38
4. Donovan DT, Conley JJ. **Capsular significance in parotid tumor surgery: reality and myths of lateral lobectomy.** *Laryngoscope* 1984;94:324–29
5. Dykun RJ, Deitel M, Borowy ZJ, et al. **Treatment of parotid neoplasms.** *Can J Surg* 1980;23:14–19
6. Heller KS, Attie JN. **Treatment of Warthin's tumor by enucleation.** *Am J Surg* 1988;156:294–96
7. Patey DH. **Current state of surgery of the salivary glands: a critical review** [in Italian]. *Recenti Prog Med* 1969;46:578–99
8. Witt RL. **The significance of the margin in parotid surgery for pleomorphic adenoma.** *Laryngoscope* 2002;112:2141–54
9. Boccato P, Altavilla G, Blandamura S. **Fine-needle aspiration biopsy of salivary gland lesions: a reappraisal of pitfalls and problems.** *Acta Cytol* 1998;42:888–98
10. Elagoz S, Gulluoglu M, Yilmazbayhan D, et al. **The value of fine-needle aspiration cytology in salivary gland lesions, 1994–2004.** *ORL J Otorhinolaryngol Relat Spec* 2007;69:51–56
11. Ivanova S, Slobodnikova J, Janska E, et al. **Fine needle aspiration biopsy in a**

diagnostic workup algorithm of salivary gland tumors. *Neoplasma* 2003;50: 144–47
12. Mihashi H, Kawahara A, Kage M, et al. **Comparison of preoperative fine-needle aspiration cytology diagnosis and histopathological diagnosis of salivary gland tumors.** *Kurume Med J* 2006;53:23–27
13. Wong DS, Li GK. **The role of fine-needle aspiration cytology in the management of parotid tumors: a critical clinical appraisal.** *Head Neck* 2000;22: 469–73
14. Das DK, Petkar MA, Al-Mane NM, et al. **Role of fine needle aspiration cytology in the diagnosis of swellings in the salivary gland regions: a study of 712 cases.** *Med Princ Pract* 2004;13:95–106
15. Behzatoglu K, Bahadir B, Kaplan HH, et al. **Fine needle aspiration biopsy of the parotid gland: diagnostic problems and 2 uncommon cases.** *Acta Cytol* 2004;48:149–54
16. Donath K, Seifert G. **Tumour-simulating squamous cell metaplasia (SCM) in necrotic areas of salivary gland tumours.** *Pathol Res Pract* 1997;193:689–93
17. Eida S, Ohki M, Sumi M, et al. **MR factor analysis: improved technology for the assessment of 2D dynamic structures of benign and malignant salivary gland tumors.** *J Magn Reson Imaging* 2008;27:1256–62
18. Eida S, Sumi M, Sakihama N, et al. **Apparent diffusion coefficient mapping of salivary gland tumors: prediction of the benignancy and malignancy.** *AJNR Am J Neuroradiol* 2007;28:116–21
19. Habermann CR, Gossrau P, Graessner J, et al. **Diffusion-weighted echo-planar MRI: a valuable tool for differentiating primary parotid gland tumors?** *Rofo* 2005;177:940–45
20. Mascaro L, Ferrari C, Grazioli L, et al. **T2 relaxation of the parotid gland of patients affected by pleomorphic adenoma.** *Magn Reson Imaging* 1999;17: 723–30
21. Matsushima N, Maeda M, Takamura M, et al. **Apparent diffusion coefficients of benign and malignant salivary gland tumors: comparison to histopathological findings.** *J Neuroradiol* 2007;34:183–89
22. Minami M, Tanioka H, Oyama K, et al. **Warthin tumor of the parotid gland: MR-pathologic correlation.** *AJNR Am J Neuroradiol* 1993;14:209–14
23. Motoori K, Iida Y, Nagai Y, et al. **MR imaging of salivary duct carcinoma.** *AJNR Am J Neuroradiol* 2005;26:1201–06
24. Motoori K, Ueda T, Uchida Y, et al. **Identification of Warthin tumor: magnetic resonance imaging versus salivary scintigraphy with technetium-99m pertechnetate.** *J Comput Assist Tomogr* 2005;29:506–12
25. Okahara M, Kiyosue H, Hori Y, et al. **Parotid tumors: MR imaging with pathological correlation.** *Eur Radiol* 2003;13(suppl 4):L25–33
26. Prades JM, Oletski A, Faye MB, et al. **Parotid gland masses: diagnostic value of MR imaging with histopathologic correlations** [in French]. *Morphologie* 2007;91:44–51
27. Sakamoto M, Sasano T, Higano S, et al. **Usefulness of heavily T(2) weighted magnetic resonance images for the differential diagnosis of parotid tumours.** *Dentomaxillofac Radiol* 2003;32:295–99
28. Takashima S, Noguchi Y, Okumura T, et al. **Dynamic MR imaging in the head and neck.** *Radiology* 1993;189:813–21
29. Takashima S, Wang J, Takayama F, et al. **Parotid masses: prediction of malignancy using magnetization transfer and MR imaging findings.** *AJR Am J Roentgenol* 2001;176:1577–84
30. Yabuuchi H, Fukuya T, Tajima T, et al. **Salivary gland tumors: diagnostic value of gadolinium-enhanced dynamic MR imaging with histopathologic correlation.** *Radiology* 2003;226:345–54
31. Yoshino N, Yamada I, Ohbayashi N, et al. **Salivary glands and lesions: evaluation of apparent diffusion coefficients with split-echo diffusion-weighted MR imaging—initial results.** *Radiology* 2001;221:837–42
32. Motoori K, Yamamoto S, Ueda T, et al. **Inter- and intratumoral variability in magnetic resonance imaging of pleomorphic adenoma: an attempt to interpret the variable magnetic resonance findings.** *J Comput Assist Tomogr* 2004;28:233–46
33. Thoeny HC, De Keyzer F, Claus FG, et al. **Gustatory stimulation changes the apparent diffusion coefficient of salivary glands: initial experience.** *Radiology* 2005;235:629–34
34. Le Bihan D, Breton E, Lallemand D, et al. **Separation of diffusion and perfusion in intravoxel incoherent motion MR imaging.** *Radiology* 1988;168:497–505
35. Matsuura H. **Surgery for pleomorphic adenoma of the parotid gland evaluated by long term follow-up** [in Japanese]. *Nippon Geka Gakkai Zasshi* 1989;90: 1386–88
36. Sciubba JJ, Brannon RB. **Myoepithelioma of salivary glands: report of 23 cases.** *Cancer* 1982;49:562–72
37. Batori M, Mariotta G, Giovannone G, et al. **Warthin's tumor of parotid gland: treatment of a retroneural lesion by enucleation.** *Eur Rev Med Pharmacol Sci* 2002;6:105–11
38. Ikeda M, Motoori K, Hanazawa T, et al. **Warthin tumor of the parotid gland: diagnostic value of MR imaging with histopathologic correlation.** *AJNR Am J Neuroradiol* 2004;25:1256–62
39. Thoeny HC. **Imaging of salivary gland tumours.** *Cancer Imaging* 2007;7:52–62